



جامعة الملك عبد الله
للعلوم والتقنية

King Abdullah University of
Science and Technology

Metal-ligand interface in the chemical reactions of ligand protected noble metal clusters

Item Type	Article
Authors	Krishnadas, Kumaranchira Ramankutty; Natarajan, Ganapati; Baksi, Ananya; Ghosh, Atanu; Khatun, Esma; Pradeep, Thalappil
Citation	Krishnadas KR, Natarajan G, Baksi A, Ghosh A, Khatun E, et al. (2018) Metal-ligand interface in the chemical reactions of ligand protected noble metal clusters. Langmuir. Available: http://dx.doi.org/10.1021/acs.langmuir.8b03493 .
Eprint version	Post-print
DOI	10.1021/acs.langmuir.8b03493
Publisher	American Chemical Society (ACS)
Journal	Langmuir
Rights	This document is the Accepted Manuscript version of a Published Work that appeared in final form in Langmuir, copyright © American Chemical Society after peer review and technical editing by the publisher. To access the final edited and published work see https://pubs.acs.org/doi/10.1021/acs.langmuir.8b03493 .
Download date	09/08/2022 08:44:35
Link to Item	http://hdl.handle.net/10754/630269

LANGMUIR

Subscriber access provided by King Abdullah University of Science and Technology Library

Invited Feature Article

Metal-ligand interface in the chemical reactions of ligand protected noble metal clusters

Kumaranchira Ramankutty Krishnadas, Ganapati Natarajan, Ananya Baksi, Atanu Ghosh, Esmā Khatun, and Thalappil Pradeep

Langmuir, **Just Accepted Manuscript** • DOI: 10.1021/acs.langmuir.8b03493 • Publication Date (Web): 06 Dec 2018

Downloaded from <http://pubs.acs.org> on December 11, 2018

Just Accepted

“Just Accepted” manuscripts have been peer-reviewed and accepted for publication. They are posted online prior to technical editing, formatting for publication and author proofing. The American Chemical Society provides “Just Accepted” as a service to the research community to expedite the dissemination of scientific material as soon as possible after acceptance. “Just Accepted” manuscripts appear in full in PDF format accompanied by an HTML abstract. “Just Accepted” manuscripts have been fully peer reviewed, but should not be considered the official version of record. They are citable by the Digital Object Identifier (DOI®). “Just Accepted” is an optional service offered to authors. Therefore, the “Just Accepted” Web site may not include all articles that will be published in the journal. After a manuscript is technically edited and formatted, it will be removed from the “Just Accepted” Web site and published as an ASAP article. Note that technical editing may introduce minor changes to the manuscript text and/or graphics which could affect content, and all legal disclaimers and ethical guidelines that apply to the journal pertain. ACS cannot be held responsible for errors or consequences arising from the use of information contained in these “Just Accepted” manuscripts.

Metal-ligand interface in the chemical reactions of ligand protected noble metal clusters

Kumaranchira Ramankutty Krishnadas,[#] Ganapati Natarajan, Ananya Baksi,[†] Atanu Ghosh,[‡] Esma Khatun and Thalappil Pradeep*

Department of Chemistry, DST Unit of Nanoscience (DST UNS) and Thematic Unit of Excellence (TUE)

Indian Institute of Technology Madras

Chennai, 600 036, India

*E-mail: pradeep@iitm.ac.in. Fax: +91-44-2257-0545.

ABSTRACT

We discuss the role of the metal-ligand (M-L) interfaces in the chemistry of ligand protected, atomically precise noble metal clusters, a new and expanding family of nanosystems, in solution as well as in gas phase. A few possible mechanisms in which the structure and dynamics of M-L interfaces could trigger intercluster exchange reactions are presented first. How interparticle chemistry can be a potential mechanism of Ostwald ripening, a well-known particle coarsening process, is also discussed. Reaction of $\text{Ag}_{59}(\text{2,5-DCBT})_{32}$ (DCBT = dichlorobenzenethiol) with 2,4-DCBT leading to the formation of $\text{Ag}_{44}(\text{2,4-DCBT})_{30}$ is presented, demonstrating the influence of the ligand structure in ligand-induced chemical transformations of clusters. We also discuss structural isomerism of clusters such as $\text{Ag}_{44}(\text{SR})_{30}$ (-SR = alkyl/aryl thiolate) in gas phase wherein

1
2
3 the occurrence of isomerism is attributed to the structural rearrangements in the M-L bonding
4 network. Interfacial bonding between $\text{Au}_{25}(\text{SR})_{18}$ clusters leading to the formation of cluster
5 dimers and trimers is also discussed. Finally, we show that desorption of phosphine and hydride
6 ligands on a silver cluster, $[\text{Ag}_{18}(\text{TPP})_{10}\text{H}_{16}]^{2+}$ (TPP = triphenylphosphine) in gas phase, lead to
7 the formation of a naked silver cluster of precise nuclearity, such as Ag_{17}^+ . We demonstrate that
8 the nature of the M-L interfaces, *i.e.*, the oxidation state of metal atoms, structure of the ligand,
9 M-L bonding network, *etc.*, play key roles in the chemical reactivity of clusters. The structure,
10 dynamics and chemical reactivity of nanosystems in general are to be explored together to obtain
11 new insights into their emerging science.
12
13
14
15
16
17
18
19
20
21
22
23
24

25 **Introduction**

26
27
28
29 Metal-ligand (M-L) interfaces play key roles in dictating the physical properties, chemical
30 reactivity and interparticle interactions of ligand protected metal nanosystems. Atomically
31 precise noble metal clusters,^{1,2} such as $\text{Au}_{102}(\text{SR})_{44}$,³ $\text{M}_{25}(\text{SR})_{18}$ (M=Ag/Au),⁴⁻⁵ $\text{Ag}_{44}(\text{SR})_{30}$,⁶⁻⁷ *etc.*
32 (–SR = alkyl/aryl thiolate), serve as convenient models to investigate the properties of M-L
33 interfaces owing to their well-defined compositions, structures and molecule-like properties.⁸⁻¹⁰
34 Such clusters have a well-defined metal core protected by a ligand shell. Feasibility to
35 incorporate a variety of ligands such as phosphines,¹¹⁻¹³ thiols,^{7, 14-19} selenols,²⁰⁻²² alkynes,²³ *etc.*,
36 also make them suitable systems to study M-L interfaces. Early in the literature, these clusters
37 were referred to as “monolayer protected clusters”,²⁴ assuming that the ligands form an extended,
38 ordered layer on particle surfaces,²⁵ which in turn resemble crystallographic planes of the
39 corresponding metals. Single crystal X-ray crystallography revealed that the M-L interfaces in
40 many of these clusters, assume well-defined, short M_xL_y oligomeric units. For example,
41
42
43
44
45
46
47
48
49
50
51
52
53
54
55
56
57
58
59
60

1
2
3 Au₂₅(SR)₁₈ is composed of a Au₁₃ core and six Au₂(SR)₃ units, often referred to as staple motifs.
4
5 Similarly, Ag₄₄(SR)₃₀ consists of an Ag₃₂ core protected by six Ag₂(SR)₅ mounts. This structural
6
7 model has been referred to as the ‘divide and protect’ model²⁶ wherein these clusters are viewed
8
9 as a core containing a precise number of metal atoms protected by a specific number of M_xL_y
10
11 oligomeric units. Structural correlations between these clusters and that of M-L complexes and
12
13 self-assembled monolayers have also been identified.²⁷ Recently, a few other structural models²⁸⁻
14
15 ³⁰in which these clusters have been considered as interlocked rings, instead of distinct staples or
16
17 mounts, have been proposed to understand the properties of these clusters. Irrespective of the
18
19 structural model, the actual structure of the ligands, their spatial distribution on the cluster
20
21 surface, binding modes of the ligands with the metal atoms, oxidation states of metal atoms, *etc.*,
22
23 need to be considered in order to understand the M-L interfaces in these clusters.
24
25
26
27
28

29 The nature of ligands such as the type of the tail groups (alkyl, aryl, *etc.*) and the
30
31 positions³¹(ortho, meta and para) of functional groups (-CH₃, -COOH, *etc.*) in them drastically
32
33 influence the nuclearity, geometry, solubility and other properties of clusters.³²⁻³³ Weak van der
34
35 Waals and/or π - π interactions between the ligands is shown to be responsible for their chiroptical
36
37 properties,³⁴⁻³⁵ supramolecular interactions,³⁶ and cluster assemblies.³⁷⁻³⁹ Electronic interaction
38
39 between the ligands and the metal core influences optical absorption⁴⁰, and luminescence⁴¹⁻⁴²
40
41 features. Metal atoms in the staples serve as the true catalytic sites in such clusters. A variety of
42
43 chemical transformations of these clusters such as ligand exchange,⁴³⁻⁴⁷ metal atom
44
45 substitution⁴⁸⁻⁵³, ligand-induced core etching⁵⁴⁻⁵⁵ and core transformation,⁵⁶⁻⁵⁸ *etc.*, were reported
46
47
48 in the last few years. Recently, reactions between clusters in solution phase were also reported.⁵⁹⁻
49
50
51
52 ⁶⁴ These reactions invariably involve the metal atoms and ligands in the staple or mount motifs of
53
54 these clusters.⁶⁵⁻⁶⁸ Dynamic nature of the staple motifs or mounts⁶⁹⁻⁷⁴ and reactions of these
55
56
57
58
59
60

1
2
3 clusters have been studied, mostly in the solution phase. Gas phase stability, dynamics of these
4
5 M-L interfaces and resulting chemical reactivity of ligand protected clusters remain poorly
6
7 understood. In order to understand the chemical reactivity of these clusters, a better
8
9 understanding of their M-L interfaces is essential.
10
11

12
13 In this *Feature* article, we discuss the role of M-L interfaces in dictating the solution as well as
14
15 gas phase reactions of ligand protected atomically precise noble metal clusters. We discuss the
16
17 role of the staples or mount motifs in such clusters in triggering the intercluster exchange
18
19 reactions. We propose that interparticle chemistry, as demonstrated between atomically precise
20
21 clusters, can be helpful to understand the chemical events behind Ostwald ripening, a well-
22
23 known particle coarsening process. Next, we show that ligand-induced transformation of
24
25 $\text{Ag}_{59}(\text{2,5-DCBT})_{32}$ to $\text{Ag}_{44}(\text{2,4-DCBT})_{30}$ (DCBT = dichlorobenzenethiol) occurs in solution
26
27 phase through the dissociation of metal ligand fragments.⁷⁵ Then we discuss three examples
28
29 wherein gas phase dynamics and reactivity of M-L interfaces are demonstrated. We present ion
30
31 mobility mass spectrometric studies showing that ligand protected clusters such as $\text{Ag}_{44}(\text{SR})_{30}$
32
33 exhibit structural isomerism in gas phase wherein the isomerism is attributed to the structural
34
35 rearrangements in the metal-ligand bonding network.⁷⁶ Interfacial bonding between $\text{Au}_{25}(\text{SR})_{18}$
36
37 clusters leading to the formation of cluster dimers and trimers is also presented.⁷⁷ Finally, we
38
39 show that desorption of phosphine and hydride ligands on a silver cluster, $[\text{Ag}_{18}(\text{TPP})_{10}\text{H}_{16}]^{2+}$ in
40
41 gas phase, lead to the formation of naked silver clusters of specific nuclearity, such as Ag_{17}^{+} .⁷⁸
42
43 We conclude the article with a summary and brief discussion of the future perspectives.
44
45
46
47
48
49
50
51
52
53
54
55
56
57
58
59
60

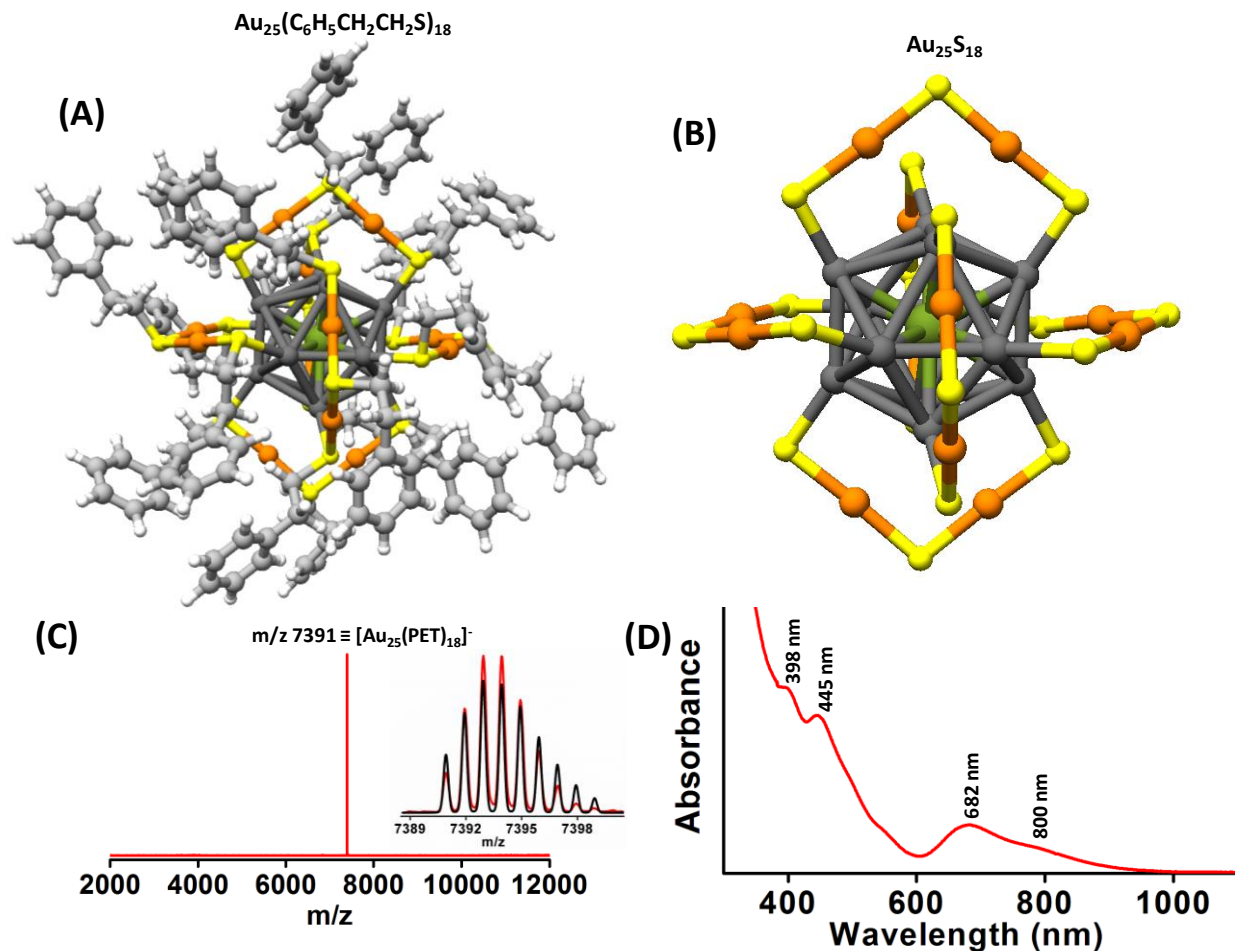


Figure 1. Crystal structure of $\text{Au}_{25}(\text{C}_6\text{H}_5\text{CH}_2\text{CH}_2\text{S})_{18}$ (A), schematic showing the icosahedral core and the six $\text{Au}_2(\text{SR})_3$ staples (B), negative ion ESI MS spectrum (C) and UV/Vis absorption spectrum of $\text{Au}_{25}(\text{C}_6\text{H}_5\text{CH}_2\text{CH}_2\text{S})_{18}$ (D). The $\text{C}_6\text{H}_5\text{CH}_2\text{CH}_2$ groups of the ligands are omitted in (B), for clarity. The figures are intended to highlight the ligand-core interface. Color codes of atoms: Au atoms in the icosahedral core (black), in the center of Au_{13} icosahedron (Green), in the staples (Orange), sulfur (Yellow), carbon (Grey) and hydrogen (White). Distinct features in the mass and the UV/Vis spectra are also marked in (C) and (D). Isotopic resolution of the molecular ion feature of $\text{Au}_{25}(\text{C}_6\text{H}_5\text{CH}_2\text{CH}_2\text{S})_{18}$ at m/z 7391 is shown in the inset of (C) along with a comparison of the theoretical (black) and experimental (red) spectrum.

Intercluster reactions: What is the role of metal ligand interface?

As mentioned above, thiolate-protected noble metal clusters have traditionally been viewed as composed of a core consisting of a definite core of metal atoms, protected with a well-defined shell of metal-ligand oligomeric complexes. Single crystal X-ray crystallographic structure of $\text{Au}_{25}(\text{C}_6\text{H}_5\text{CH}_2\text{CH}_2\text{S})_{18}$, for example, is shown in Figures 1A and 1B. This cluster consists of an inner Au_{12} icosahedral core (black spheres in Figures 1A and 1B) encapsulating a central Au atom (green spheres in Figures 1A and 1B) and the ligands are distributed in six, distinct $\text{Au}_2(\text{SR})_3$ staple motifs (see orange and yellow spheres in Figure 1B). The composition and charge state of these clusters are further confirmed through electrospray ionization mass spectrometry (ESI MS) as well, as shown in Figure 1C. High resolution spectrum shows the isotopic features. Although Au has only one isotope, the isotopes of S (^{32}S , ^{33}S , ^{34}S and ^{36}S), C (^{12}C and ^{13}C) and H (^1H and ^2H) produce a rich spectrum. Such richness can be used to confirm the composition of the cluster by comparing with the theoretical spectrum. Electronic structure calculations show that the distinct electronic absorption features of these clusters (see Figure 1D) originate from various transitions in their discrete electronic energy levels. Thus, crystallography and electronic structure calculations support this structural model of these ligand-protected noble metal clusters. However, in order to understand the chemical reactivity of these clusters, it is necessary to consider other structural models. We discuss some of these aspects in the preceding sections.

Recently, intercluster reactions, resulting in the exchange of metal atoms, ligands and metal ligand fragments between them have been demonstrated.^{59-60, 62-63} However, the mechanisms of such reactions, especially how such reactions are triggered, remain unknown. In this section, we discuss a few possible ways by which the structure and dynamics of M-L interfaces trigger

1
2
3 intercluster reactivity. For this, we consider the reaction between two structurally and
4
5 compositionally analogous noble metal clusters, $\text{Ag}_{25}(\text{SR})_{18}$ and $\text{Au}_{25}(\text{SR})_{18}$.⁵⁹ As mentioned
6
7 above, these clusters have traditionally been viewed as composed of a distinct M_{13} core protected
8
9 by $\text{M}_2(\text{SR})_3$ ($\text{M} = \text{Ag}/\text{Au}$) staples. According to the superatom theory,²⁷ valence electrons of
10
11 metal atoms in their staples are localized by polar covalent bonds with sulfur atom of the ligands.
12
13 Furthermore, each of the $\text{M}_2(\text{SR})_3$ staples localizes the valence electron of one of the metal atoms
14
15 in the M_{13} core. Therefore, all of the metal atoms in the six $\text{M}_2(\text{SR})_3$ staples and six of the metal
16
17 atoms in the M_{13} core are considered to be in +1 oxidation state. The remaining seven electrons
18
19 and an acquired negative charge make the eight electron superatom, $[\text{Au}_{25}(\text{SR})_{18}]^-$. In the crystal
20
21 structure, the charge neutrality is provided by the metal ions or ammonium ions. The studies
22
23 presented in this article are performed with this $\text{Au}_{25}(\text{SR})_{18}$ anions in solution, although this may
24
25 not be mentioned explicitly.
26
27
28
29
30

31
32 We think that the difference in the oxidation states of metal atoms in the core and the staples,
33
34 as explained above, play a crucial role in triggering the intercluster reactions. Because of this
35
36 difference in oxidation states, redox-like reactions could occur between two clusters. Let us
37
38 consider two such possibilities, taking the reaction between $\text{Ag}_{25}(\text{SR})_{18}$ and $\text{Au}_{25}(\text{SR})_{18}$ as an
39
40 example. In the first case, an $\text{Ag}_{25}(\text{SR})_{18}$ molecule reacts with the $\text{Au}_2(\text{SR})_3$ staples of the
41
42 $\text{Au}_{25}(\text{SR})_{18}$, wherein Au of $\text{Au}_2(\text{SR})_3$ staples is in +1 oxidation state. Note that redox reactions
43
44 between silver clusters and Au(I)-thiolates are known.⁷⁹ Alternatively, an $\text{Au}_{25}(\text{SR})_{18}$ molecule
45
46 reacts with the $\text{Ag}_2(\text{SR})_3$ staples of the $\text{Ag}_{25}(\text{SR})_{18}$, wherein Ag of $\text{Ag}_2(\text{SR})_3$ staple is in +1
47
48 oxidation state. Such reactions between $\text{Au}_{25}(\text{SR})_{18}$ and Ag(I)-thiolates are also known.⁸⁰ It
49
50 remains still unclear how the difference in oxidation states of metal atoms in the core and the
51
52 staples contributes to the chemical reactivity of these clusters. Apart from these possibilities, it
53
54
55
56
57
58
59
60

1
2
3 has also been intuitively suggested in the reaction between $\text{Au}_{25}(\text{SR})_{18}$ and $\text{Ag}_{44}(\text{SR})_{30}$ that the
4
5 interaction between these two intact clusters could result in the formation of small, reactive
6
7 fragments such as $\text{Ag}(\text{SR})_2^-$ which react with the $\text{Au}_2(\text{SR})_3$ staples of $\text{Au}_{25}(\text{SR})_{18}$ resulting in
8
9 exchange of metal atoms, ligands and M-L fragments.⁶² In this context, it is important to
10
11 understand how far the chemistry of these clusters differ from that of the M-L complexes. In
12
13 other words, do these clusters behave as unique entities in their reactions wherein the overall
14
15 electronic structures of both of the reacting clusters need to be considered in order to explain
16
17 their reactivity (rather than attributing their chemistry as due to the reaction between one of the
18
19 clusters and the staples or the mounts of the other, as explained earlier)?
20
21
22
23

24
25 A new structural model, namely, the Borromean rings model,²⁸ has been proposed for the
26
27 noble metal cluster $\text{Au}_{25}(\text{SR})_{18}$ by Natarajan *et al.*, wherein $\text{Au}_{25}(\text{SR})_{18}$, has been considered as
28
29 part of three interlocked $\text{Au}_8(\text{SR})_6$ rings surrounding the central Au atoms (see Figure 2). In this,
30
31 all the metal and sulfur atoms, except the central metal atom, belong to a unique structural
32
33 component, the $\text{Au}_8(\text{SR})_6$ ring. This model suggests that disconnecting any ring leads to two
34
35 unlinked rings, which is a defining characteristic of the Borromean rings bonding topology (see
36
37 Figure 2B). The Borromean rings model also applies to a silver cluster, $\text{Ag}_{25}(\text{SR})_{18}$, which is a
38
39 structural analogue of $\text{Au}_{25}(\text{SR})_{18}$. Natarajan *et al.*, also noted that interlocked metal-thiolate ring
40
41 structures have been found in the core and staple structures of a few gold-thiolate clusters which
42
43 have crystal structures available, both smaller and larger than $\text{Au}_{25}(\text{SR})_{18}$, namely
44
45 $\text{Au}_{10}(\text{SR})_{10}$,⁸¹ $\text{Au}_{20}(\text{SR})_{16}$ ⁸² and $\text{Au}_{144}(\text{SR})_{60}$ ^{30, 83}. They suggested that the interlocked ring
46
47 structures form a strong framework for the clusters and may possibly represent a unified
48
49 viewpoint for the structure of monolayer protected clusters. According to this interlocked-ring
50
51 structural model, these clusters being formed out of and stabilized by ring structures, are more
52
53
54
55
56
57
58
59
60

1
2
3 dynamic in nature than one would expect from the core/staple model, because in the latter, the
4
5 M_{13} core has been viewed as distinct, compact structural unit which is difficult to undergo any
6
7 structural distortion. Furthermore, if the cluster existed in solution as distinct, structurally rigid
8
9 Au_{13} core and $Au_2(SR)_3$ staples, exchange of metal atoms into the core would not have been
10
11 feasible. However, exchange of metal atoms in the core also occurs during the reaction between
12
13 $Ag_{25}(SR)_{18}$ and $Au_{25}(SR)_{18}$ suggesting that the icosahedral Au_{13} core is flexible and dynamic in
14
15 nature, as experimentally proven by Tsukuda *et al.*²⁹ Ghosh *et al.* have shown that dynamics of
16
17 M-L interfaces can be controlled by using dithiolates which bind to the metal core in a bidentate
18
19 fashion and thereby reducing the flexibility of the metal-ligand bonding network.⁸⁴ Hence, we
20
21 think that an interlocked-ring model of the structure can better explain the enhanced dynamics of
22
23 M-L interfaces and reactivity of clusters.
24
25
26
27
28

29
30 Even though the mechanistic details are not known, it has been suggested that interactions
31
32 between the M-L interfaces might occur in the initial stages of these reactions. In the reaction
33
34 between $Au_{25}(SR)_{18}$ and $Ag_{25}(SR)_{18}$, we detected a dimeric species,
35
36 $[Ag_{25}Au_{25}(DMBT)_{18}(PET)_{18}]^{2-}$, which could be one of the intermediates of the reaction.⁵⁶ DFT
37
38 calculations revealed that this adduct could be formed through a weak covalent bonding between
39
40 them through inter-staple metal sulfur bonds.⁵⁹ Recently, Zhang *et al.*, attempted to detect such
41
42 intermediates during the reaction between $Au_{38-x}Ag_x(SR)_{24}$ and $Au_{38}(SR)_{24}$ using *in situ* X-ray
43
44 absorption fine structure (XAFS) measurements.⁶⁶ However, detection of exchanged Ag atoms in
45
46 the staples was not successful, possibly due to shorter residence time of the exchanged Ag atoms
47
48 in the staples.
49
50
51
52
53
54
55
56
57
58
59
60

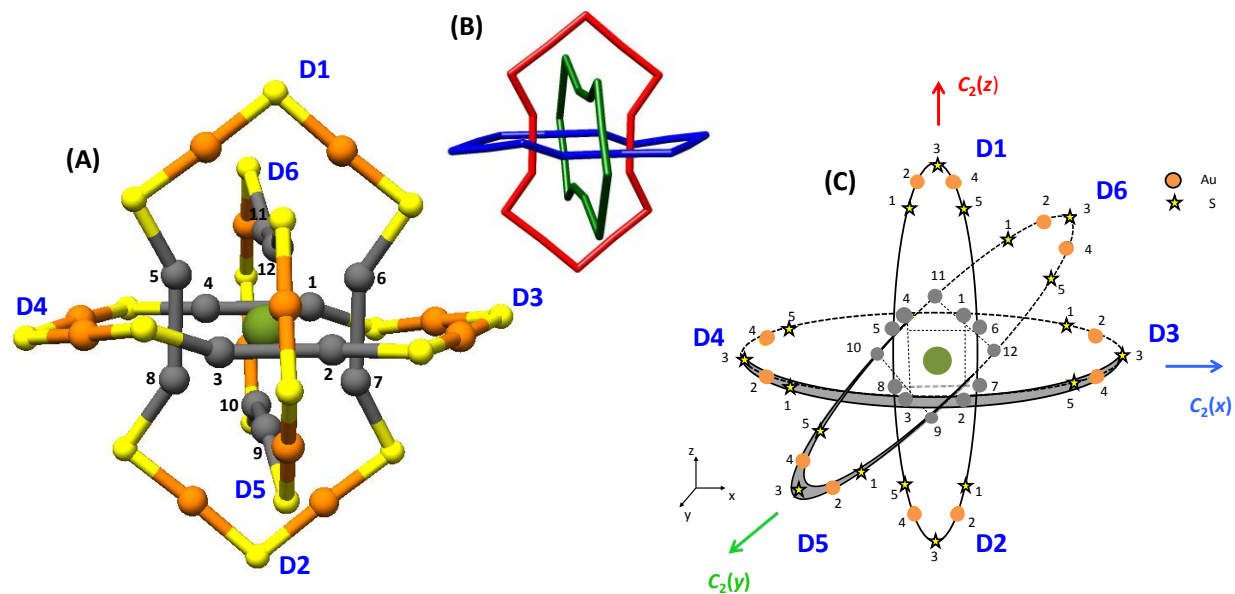


Figure 2. (A) A visualization of $\text{Au}_{25}\text{S}_{18}$ as the ring structure consisting of three interlocked (Au_8S_6) -rings. (B) The topological configuration of the Borromean rings, with the three rings Au_8S_6 rings being colored red, blue and green. (C) A 2D schematic diagram of the Borromean rings formed by planar-projection of the $\text{Au}_{25}\text{S}_{18}$ ring structure shown in (A), wherein the Au_8S_6 rings formed by pairs of coplanar staples are shown as ellipses. Gold atoms in the icosahedral core are shown by grey circles and yellow stars represent the positions of S atoms of the thiolate ligand. The core Au atoms are numbered from 1 to 12 and the staple atoms are numbered clockwise from end of the staple, from 1 to 5. The lines that join core Au atoms on opposite ends of the same staple are shown by the dotted lines. The three perpendicular C_2 axes are marked with the associated Cartesian axes directions in brackets. The staple directions are labeled by the six staple locants D1 to D6, marked in blue. In each Au_8S_6 ring, there are three sets of coplanar staples, *i.e.*, D1-D2, D3-D4 and D5-D6. Color codes of atoms in (A): Au atoms in the icosahedral core (grey), centre of the Au_{13} icosahedron (Green), staples (Orange), Sulfur (Yellow). (Adapted with permission from, Ref. 28)

Ostwald ripening and interparticle reactions

Ostwald ripening is one of the important mechanisms of nanocrystal growth⁸⁵ wherein larger particles grow larger at the expense of smaller ones in solution. Thermodynamic driving force behind this process is the difference in surface energies of (smaller and larger) particles in a polydisperse solution/dispersion. Smaller particles possess higher surface energy and hence, they disappear more easily compared to the larger particles in the same solution/dispersion. Ostwald ripening occurs by the diffusion of the smaller particles, towards the larger particles and subsequent reactions between them resulting in the growth of the particle.⁸⁵ This makes the larger particles grow larger in size, consuming or reducing the size of the smaller ones. However, it remains unclear how the constituents (atoms, ions or molecules) of smaller particles are transported to the larger ones, *i.e.*, by a direct interparticle exchange or exchange of their fragments, in such processes. Details of chemical events in such processes are not known clearly. It was shown that in the case of noble metal clusters, exchanges of metal atoms, ligands and metal ligand fragments occur through direct interaction or collision between the reacting clusters. How do these two processes *i.e.*, intercluster exchange and Ostwald ripening, differ from each other? Can Ostwald ripening be interpreted or understood as interparticle exchange reactions between larger particles and smaller ones?

Let us discuss this briefly in the context of ligand protected metal nanosystems. For example, consider a dispersion of thiolate-protected metal nanoparticles, which are typically polydisperse in their sizes. In such a mixture, smaller particles could be more reactive compared to the larger ones, also for reasons other than the surface energy differences, such as change in the oxidation states, differences in the redox potentials of (smaller and larger) particles, differences in metal-ligand binding modes, *etc.* as mentioned previously in the context of atomically precise clusters.

1
2
3 Do such factors contribute to the interparticle reactions (between larger and smaller particles)
4
5 resulting in Ostwald ripening?
6
7

8
9 In the intercluster exchange reactions reported so far, the size, structure, composition (*i.e.*,
10 number of metal atoms and ligands) and charge state remain unaltered. This could be due to the
11 tendency of these clusters to retain their compact, highly symmetric, geometrically and
12 electronically stable structures. Furthermore, these clusters are molecule-like and are of
13 comparable sizes wherein electronic factors, such as shell closing effects, rather than geometrical
14 factors determine the stability. However, in Ostwald ripening, particle size changes, as
15 mentioned above. In this context, it is interesting to check whether there is a clear particle size
16 limit, at which an intercluster/interparticle exchange reaction and an Ostwald ripening can be
17 discriminated by the change or constancy of the particle size? Maran *et al.*, have recently
18 reported the formation of Au₃₈(SR)₂₄ from a smaller cluster, Au₂₅(SR)₁₈ which they referred to as
19 “gold fusion”. However, it remains unclear whether this reaction can be understood as an
20 example of Ostwald ripening of atomically precise clusters.⁸⁶ The above discussion imply that it
21 is important to investigate what are the (surface/interfacial) chemical events *between* particles in
22 an Ostwald ripening process, at least in the context of ligand protected nanosystems.
23
24
25
26
27
28
29
30
31
32
33
34
35
36
37
38
39
40

41 **Ligand’s influence on cluster transformations**

42
43
44

45 Atomically precise clusters of a wide variety of nuclearity, geometry and protecting ligands are
46 reported in the last decade. However, it remains unknown how the actual structure of the ligands
47 influences the nuclearity and geometry of the clusters. One of the ways to investigate this aspect
48 is to study the reactions of ligand protected clusters with free ligands. Often, exchange of ligands
49 occurs in these reactions without altering the overall structure and charge states of the clusters.⁴⁵⁻
50
51
52
53
54
55
56
57
58
59
60

1
2
3 ^{47, 87} However, in some cases, reactions of a cluster with a new type of ligand transforms the
4
5 cluster to completely new entities.^{53, 88}
6
7

8
9 Khatun *et al.* demonstrated that such a reaction wherein a monothiolate protected cluster, Ag₅₉
10 upon the reaction with 2,4-DCBT ligand, slowly converts it to Ag₄₄(DCBT)₃₀.⁷⁵ Note that the
11 ligands 2,4-DCBT and 2,5-DCBT differ only in the positions of the substituent Cl groups
12 (isomeric thiols). This reaction demonstrates that such minute changes in the structure of the
13 ligands drastically changes the nuclearity of cluster. This could be due to the position dependent
14 (ortho, para, or meta) changes in the electron donating or withdrawing inductive (+I or -I) effects
15 of the methyl groups of the ligands. The π - π interactions and steric hindrance between the
16 substituent groups might also play a role in these transformations. Mass spectrometric
17 measurements reveal that the reaction involves the formation of small metal-ligand fragments of
18 clusters (see Figure 3). Exchange of ligands were proposed to be the initial stages of such
19 transformations⁸⁹; however, in this case, no ligand exchanges were observed as the molecular
20 masses of both thiols were the same. The use of different thiol such as, FTP (4-fluorothiophenol)
21 and CTP (4-chlorothiophenol) shows ligand exchanged peaks. Another reason could be the
22 sensitivity of certain structural motifs such as staples, mounts, *etc.*, towards the structure of the
23 incoming ligands, *i.e.*, the M-L motifs may not be able to accommodate the incoming ligands
24 retaining their geometry and bonding network. Simulations and experimental techniques with
25 better temporal resolution are essential to probe such dynamics of the M-L interfaces.
26
27
28
29
30
31
32
33
34
35
36
37
38
39
40
41
42
43
44
45
46
47
48
49
50
51
52
53
54
55
56
57
58
59
60

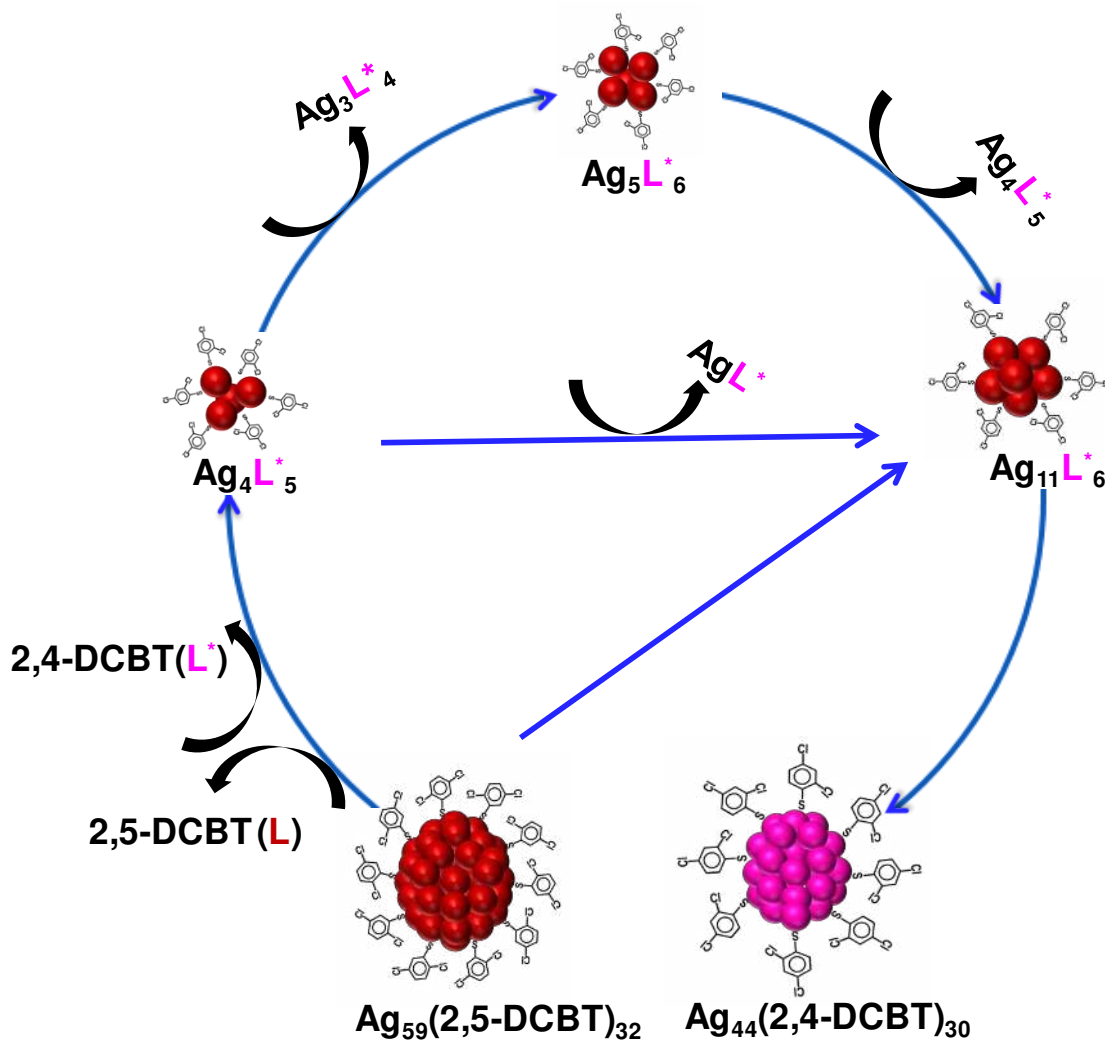


Figure 3. Schematic of the ligand-induced conversion pathway of $\text{Ag}_{59}(\text{2,5-DCBT})_{32}$ to $\text{Ag}_{44}(\text{2,4-DCBT})_{30}$. L and L* denote 2,5-DCBT and 2,4-DCBT, respectively (Reproduced with permission from, Ref. 75)

Gas phase dynamics and reactivity of M-L interfaces

Dynamics of M-L interfaces have been studied mostly in the solution phase, however, such studies of the structure, dynamics and reactivity of isolated, ligand protected metal clusters in gas phase remains largely unexplored. One of the techniques for probing the gaseous phase dynamics

1
2
3 of molecular systems is ion mobility mass spectrometry (IM MS).⁹⁰ This technique has been
4 traditionally used for gas phase analysis of small molecules⁹⁰ and conformational studies of
5 proteins;⁷⁶ however, recently, it has been utilized for probing the thiolate protected metal clusters
6 as well.⁹¹ In this technique, molecules are ionized and taken to the gaseous phase using standard
7 mass spectrometric techniques and then, they are separated according to their mobility in
8 presence of a buffer gas. The mobility of the molecules depends on their mass to charge ratio,
9 size and shape. Here we present the results of IM MS measurements of $\text{Ag}_{44}(\text{SR})_{30}$. Crystal
10 structure of $\text{Ag}_{44}(\text{SR})_{30}$ shows that it consists of a Ag_{32} core protected by six $\text{Ag}_2(\text{SR})_5$ mounts.
11 $\text{Ag}_{44}(\text{SR})_{30}$ is an interesting system in this regard because of its multi-shell structures and unusual
12 geometry of $\text{Ag}_2(\text{SR})_5$ mounts. Furthermore, this cluster occurs in different charge states in the
13 gas phase. For these experiments, $\text{Ag}_{44}(\text{SR})_{30}$ clusters were brought to the gas phase using
14 conventional electrospray ionization (ESI) technique. Ion mobility measurements on these
15 clusters reveal the presence of structural isomers, as depicted in Figure 4.⁷⁶ Here we have used a
16 model system, $\text{Ag}_{44}(\text{SH})_{30}$ to represent the structure.
17
18
19
20
21
22
23
24
25
26
27
28
29
30
31
32
33
34
35
36
37
38
39
40
41
42
43
44
45
46
47
48
49
50
51
52
53
54
55
56
57
58
59
60

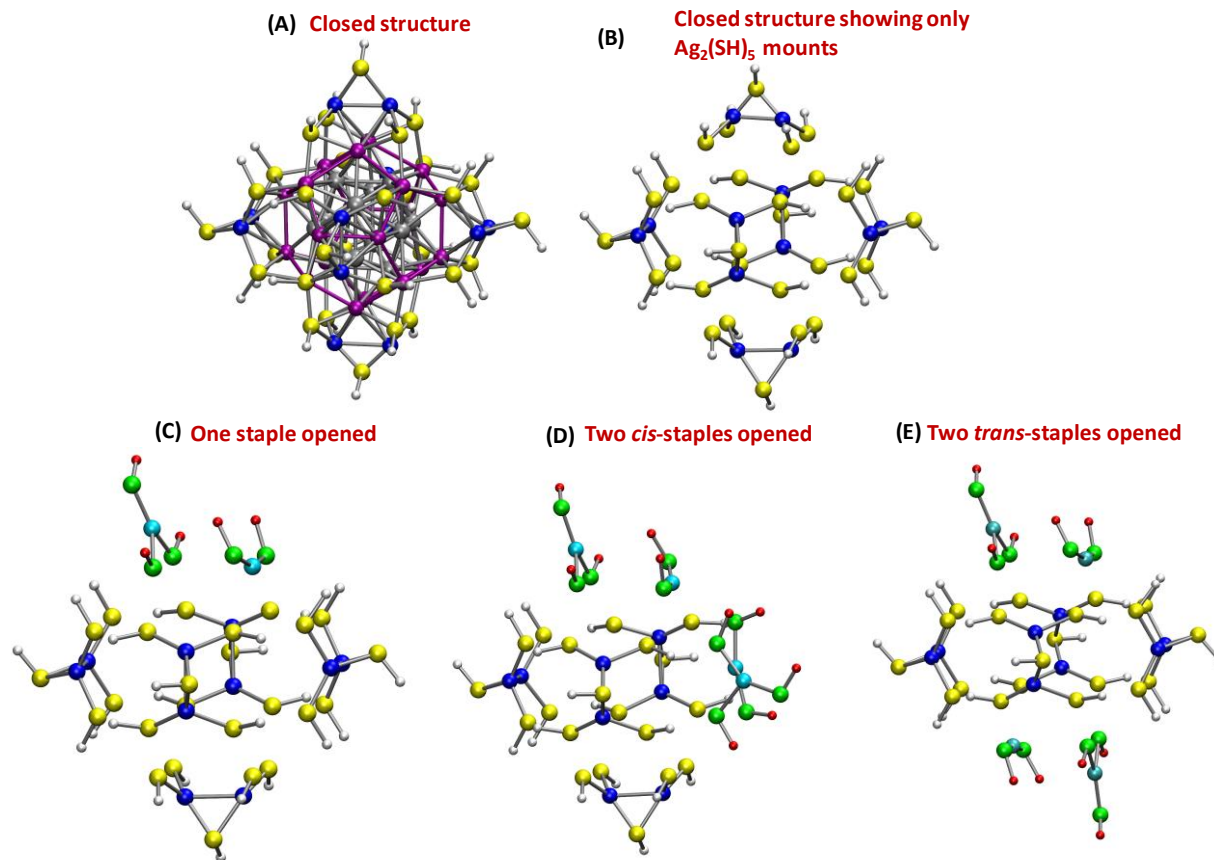


Figure 4. Schematic structures of the isomers of $[\text{Ag}_{44}(\text{SH})_{30}]^{4-}$. Geometries of $[\text{Ag}_{44}(\text{SH})_{30}]^{4-}$ with (A) and without (B) the core atoms, and its three structural isomers (C-E) with one staple opened (C), two *cis*-staples opened (D), and two *trans* staples opened (E) structures. Closed $\text{Ag}_2(\text{SH})_5$ mounts in (A)-(E) are shown in blue (silver), yellow (sulfur) and white (hydrogen) colors. Open $\text{Ag}_2(\text{SH})_5$ mounts in (C)-(E) are shown in cyan (silver), green (sulfur) and red (hydrogen) colors. Since the structure of the Ag_{12} icosahedron (gray in A) and the Ag_{20} dodecahedron (pink in A) are retained in their isomers, these core atoms are not shown in (C)-(E) for clearly distinguishing the changes in the staple arrangements in its isomers. Since the actual ligands are not shown here, additional structural isomers due to the difference in the ligand conformations are not presented here. (Adapted with permission from, Ref. 76)

1
2
3 Density functional theory (DFT) calculations suggest that the difference in the isomerism arises
4 due to the difference in the bonding network of the metal-ligand interface in these clusters. Note
5
6 that the $\text{Ag}_2(\text{SR})_5$ mounts have complicated bonding compared to those in the $\text{Au}_2(\text{SR})_3$ staples
7
8 and therefore, it is likely that some of the bonds in the $\text{Ag}_2(\text{SR})_5$ mounts could break, leading to
9
10 more stable, open structures. However, these isomers possess the same Ag_{32} core structure as in
11
12 the crystal structure. Note that these structures possess exactly the same molecular formulae,
13
14 $\text{Ag}_{44}(\text{SR})_{30}$, and differ from each other only in terms of the structures of a few of their mount
15
16 motifs and hence, they are structurally isomeric. Hence, this study reveals that rearrangements in
17
18 the metal ligand interface can generate structural isomerism in these clusters. However, if the
19
20 real ligands are involved, their confirmations also have to be taken into account when their
21
22 structural isomerism is discussed. However, such an analysis is beyond the scope of this article.
23
24
25
26
27
28

29 In another example of ion mobility mass spectrometric experiments, we show that $\text{Au}_{25}(\text{SR})_{18}$
30
31 clusters form dimers, $[\text{Au}_{50}(\text{SR})_{36}]^{2-}$, for example, and trimers in gas phase experiments. DFT
32
33 calculations show that these dimers were formed by the bonding between the $\text{Au}_2(\text{SR})_3$ staple
34
35 motifs, as shown in Figure 5.⁷⁷ Spectroscopic evidence of such bonding in gas phase is not
36
37 available so far, however, inter-staple bonding has been detected in crystals.³⁸ Note that this type
38
39 of inter-staple bonding has not altered the total number of metal atoms, ligands and the charge
40
41 states of individual clusters in these dimers. Furthermore, existence of such isomers further
42
43 support the dynamic nature of the metal ligand interface in such clusters. Also, we think that the
44
45 Borromean rings model is better suited to explain the formation of such dimers because the
46
47 longer $\text{Au}_8(\text{SR})_6$ rings are expected to be more dynamic in nature, compared to the shorter
48
49 $\text{Au}_2(\text{SR})_3$ staples, which could facilitate their breaking and reforming, leading to intercluster
50
51 bonding.
52
53
54
55
56
57
58
59
60

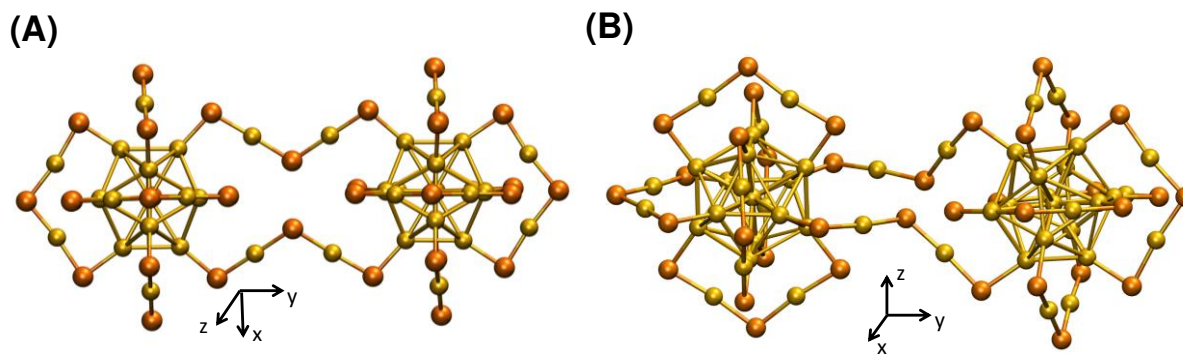
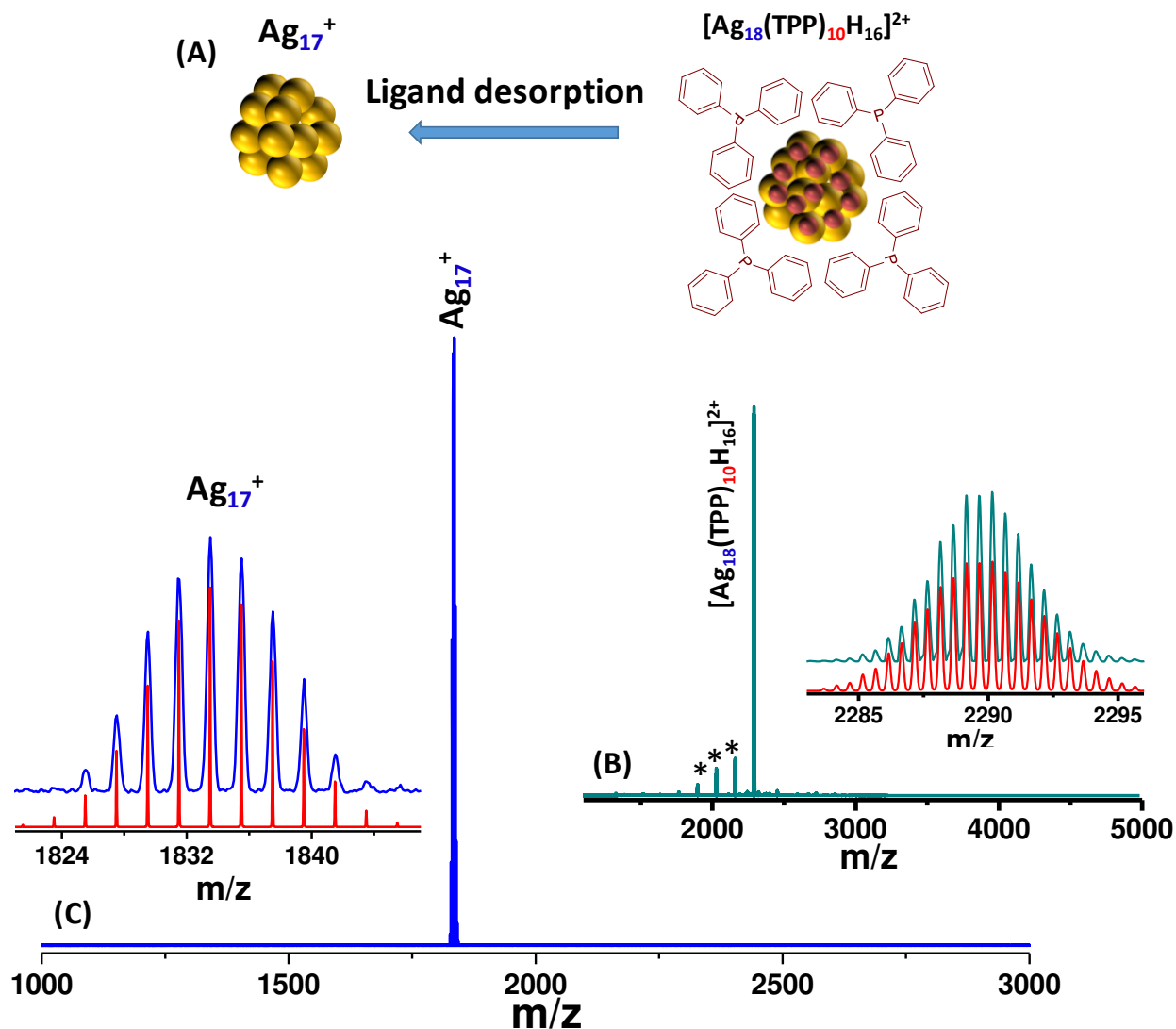


Figure 5. Interfacial bonding between clusters resulting in the formation of dimers. (A and B) DFT-optimized structures of possible structural isomers of $[\text{Au}_{50}(\text{SR})_{36}]^{2-}$ considering inter-cluster bonding via common Au_2S_3 staples. In (A), there is bonding between the two clusters by two parallel Au_2S_3 chains. The view shown is along the negative z-direction (top view). In (B), a twisted linkage between the Au_2S_3 staples of two clusters is shown with the cluster on the right being rotated by 90° anticlockwise about the x-axis, and it is coming out of the paper. Cartesian axes are shown. The ligand R-groups have been removed for clarity. Color codes of atoms: gold (orange), sulphur (yellow). (Adapted with permission from, Ref. 77)

Desorption of ligands: New route for naked metal clusters

The strength of the chemical bond between the metal atoms and the anchoring atom of the ligands (Au-S bond in $\text{Au}_{25}(\text{SR})_{18}$, for example) largely determines the stability of the clusters. Fragmentation behavior of these clusters was also studied using mass spectrometry⁹¹⁻⁹² and computations⁹³. For example, phosphines are known to bind to metal atoms less strongly, compared to thiolates, through weak covalent bonds. In this context, it is interesting to test whether it is possible to detach the ligands from phosphine protected noble metal clusters, in gaseous or liquid phase, so that naked clusters, with precise nuclearity, are generated.

Conventionally, naked metal clusters are generated by techniques such as laser ablation or electro spray which require sophisticated instrumentation for mass selection.



1
2
3 **Figure 6.** Schematic of the desorption of triphenylphosphine (TPP) ligands from
4
5 $[\text{Ag}_{18}(\text{TPP})_{10}\text{H}_{16}]^{2+}$ leading to the formation of naked, Ag_{17}^+ (A), ESI mass spectrum of
6
7 $[\text{Ag}_{18}(\text{TPP})_{10}\text{H}_{16}]^{2+}$ (B), Ag_{17}^+ (C). Insets of (B) and (C) shows the matching of the theoretical
8
9 (red) and experimental (blue in C, green in B) isotopic patterns of the corresponding ions. Color
10
11 codes of atoms in (A): silver (yellow), hydrogen (red). (Adapted with permission from, Ref. 78)

12
13
14
15
16 Ghosh *et al.*, demonstrated that it is indeed possible to generate atomically precise naked metal
17
18 clusters from a silver cluster, $[\text{Ag}_{18}(\text{TPP})_{10}\text{H}_{16}]^{2+}$, protected by phosphine and hydride ligands.
19
20 $[\text{Ag}_{18}(\text{TPP})_{10}\text{H}_{16}]^{2+}$ can be sequentially desorbed to generate naked silver clusters of specific
21
22 nuclearity, such as Ag_{17}^+ .⁷⁸ For this, $[\text{Ag}_{18}(\text{TPP})_{10}\text{H}_{16}]^{2+}$ was introduced to gas phase using an
23
24 ESI source. Sequential fragmentation of the ligands was carried out by successively increasing
25
26 the ionization voltages in the ESI set up. Figure 6 shows that $[\text{Ag}_{18}(\text{TPP})_{10}\text{H}_{16}]^{2+}$ initially
27
28 transforms to $\text{Ag}_{17}\text{H}_{14}^+$ which finally loses all the hydride ions, generating Ag_{17}^+ . Note that the
29
30 desorption of ligands in this case occurred through the breaking of the bond between the metal
31
32 and the anchoring atom of the ligand, *i.e.*, Ag-P bond. This is in contrast to the case of thiolate
33
34 protected clusters wherein the S-C bond breaks and metal-sulfur bond is retained. The formation
35
36 of naked clusters from thiolate protected clusters has never been observed. This could be
37
38 attributed to the fact that the Ag/Au-S bond is much stronger than the Ag-P bond. Similarly,
39
40 ligands such as pyridine or its analogues might also act as weaker ligands to these types of
41
42 clusters, and such systems also could lead to the formation of naked clusters. However, the
43
44 example presented above indicates that desorption of ligands depends on the nature of the
45
46 ligands as well as the strength of the bond between the metal atom and the anchoring atom of the
47
48 ligands. Such ligand desorption can occur also in ambient air, leading to naked clusters.⁹⁴
49
50
51
52
53
54
55
56
57
58
59
60

Summary and future perspectives

In summary, we presented a few examples demonstrating the role of the structure and dynamics of metal-ligand interface in dictating the chemical reactivity of monolayer protected noble metal clusters in solution as well as in the gas phase. We suggested that the difference in the oxidation states of metal atoms at the M-L interface could be a key factor triggering intercluster reaction. The structure of the M-L ligand bonding network (staples *vs* mounts, monodentate *vs* bidentate, *etc.*) and dynamics (Interlocked (Borromean) rings model *vs* core-staple model) dictate the type as well as the extent of the exchange processes. Furthermore, these studies imply that a single structural model is inadequate to explain spontaneous reactions between these clusters; consideration of multiple structural models is essential for a better understanding of their properties.

We proposed that interparticle chemistry may not be limited to metal clusters, but such reactions might also occur in other nanosystems, which could be a potential mechanism in particle coarsening processes such as Ostwald ripening. We also showed that the nature of the ligands, *i.e.*, their structure and electron donating withdrawing properties, is crucial in controlling the geometry and nuclearity of these clusters. The dynamics of the M-L interfaces is not limited to the solution phase; structural rearrangements and interfacial bonding occurs in gas phase as well, leading to the formation of geometrical isomers and cluster assemblies. Finally, we showed that the ligands can be desorbed completely in the gas phase, leading to the formation of atomically precise naked metal clusters. This study indicates that phosphines can be promising ligands for generating naked clusters of other metals as well.

1
2
3 Even though, we demonstrated that a number of factors concerning the M-L interfaces, such as
4 oxidation states of metal atoms, actual structure of the ligands, *etc.*, are important when
5
6 considering the chemistry of these clusters, contribution of each of these factors has not been
7
8 understood in isolation. Among the reasons is the limitation in making many of the clusters, by
9
10 varying only one aspect alone at one time, such as specific ligands.
11
12
13
14

15 Probing the interfacial properties for these clusters is essential for creating cluster assembled
16
17 materials and new types of hybrid materials comprising of distinctly different types of
18
19 nanosystems. Probing the kinetics and thermodynamics and real time monitoring of interfacial
20
21 phenomena in these clusters are rarely addressed. Gas phase dynamics of these clusters remain
22
23 largely unexplored. Probing the chiroptical properties of these clusters in gaseous phase could be
24
25 a potential new direction in this regard. Further efforts are needed to clearly understand the
26
27 contribution metal-ligand interfaces in dictating the geometric structures, dynamics and chemical
28
29 reactivity of ligand protected metal clusters. We think that the dynamic interfacial chemistry is
30
31 not limited to metal clusters, and hence, the structure, dynamics and chemical reactivity of
32
33 nanosystems in general are to be explored in greater detail, which might unveil new directions in
34
35 materials chemistry.
36
37
38
39
40

41 42 AUTHOR INFORMATION

43 44 **Corresponding Author**

45
46
47 *pradeep@iitm.ac.in
48
49

50 51 **Present Addresses**

52
53 #K.R.K.: Postdoctoral fellow at University of Geneva, Switzerland.
54
55

56 †A.B.: Postdoctoral fellow at Karlsruhe Institute of Technology, Germany.
57
58
59
60

1
2
3 ‡A.G.: Postdoctoral fellow at King Abdullah University of Science and Technology, Kingdom of Saudi Arabia.
4
5

6 **Author Contributions**

7
8
9 The manuscript was written through contributions of all authors. All authors have given approval
10
11 to the final version of the manuscript.
12
13

14 **Notes**

15
16
17 The authors declare no competing financial interest
18
19

20 **ACKNOWLEDGMENT**

21
22 K.R.K., A.G. and E.K. thank the UGC for their senior research fellowships. A.B. thanks IIT
23
24 Madras for an Institute Post-Doctoral Fellowship. We thank the Department of Science and
25
26 Technology for constantly supporting our research program.
27
28
29

30 **REFERENCES**

- 31
32
33 1. Jin, R.; Zeng, C.; Zhou, M.; Chen, Y. Atomically Precise Colloidal Metal Nanoclusters and
34
35 Nanoparticles: Fundamentals and Opportunities *Chem. Rev.* **2016**, *116*, 10346–10413.
36
37
38 2. Chakraborty, I.; Pradeep, T. Atomically precise clusters of noble metals: Emerging link
39
40 between atoms and nanoparticles. *Chem. Rev.* **2017**, *117*, 8208-8271.
41
42
43 3. Jadzinsky, P. D.; Calero, G.; Ackerson, C. J.; Bushnell, D. A.; Kornberg, R. D. Structure of a
44
45 thiol monolayer-protected gold nanoparticle at 1.1 Å resolution. *Science* **2007**, *318*, 430-433.
46
47
48 4. Heaven, M. W.; Dass, A.; White, P. S.; Holt, K. M.; Murray, R. W. Crystal structure of the
49
50 gold nanoparticle [N(C₈H₁₇)₄][Au₂₅(SCH₂CH₂Ph)₁₈]. *J. Am. Chem. Soc.* **2008**, *130*, 3754-3755.
51
52
53
54
55
56
57
58
59
60

- 1
2
3 5. Joshi, C. P.; Bootharaju, M. S.; Alhilaly, M. J.; Bakr, O. M. [Ag₂₅(SR)₁₈]⁻: The "Golden"
4
5 silver nanoparticle. *J. Am. Chem. Soc.* **2015**, *137*, 11578-11581.
6
7
- 8
9 6. Desireddy, A.; Conn, B. E.; Guo, J.; Yoon, B.; Barnett, R. N.; Monahan, B. M.; Kirschbaum,
10
11 K.; Griffith, W. P.; Whetten, R. L.; Landman, U.; Bigioni, T. P. Ultrastable silver nanoparticles.
12
13 *Nature* **2013**, *501*, 399-402.
14
15
- 16
17 7. Harkness, K. M.; Tang, Y.; Dass, A.; Pan, J.; Kothalawala, N.; Reddy, V. J.; Cliffler, D. E.;
18
19 Demeler, B.; Stellacci, F.; Bakr, O. M.; McLean, J. A. Ag₄₄(SR)₃₀⁴⁻: a silver-thiolate superatom
20
21 complex. *Nanoscale* **2012**, *4*, 4269-4274.
22
23
- 24
25 8. Zhu, M.; Aikens, C. M.; Hollander, F. J.; Schatz, G. C.; Jin, R. Correlating the crystal
26
27 structure of a thiol-protected Au₂₅ cluster and optical properties. *J. Am. Chem. Soc.* **2008**, *130*,
28
29 5883-5885.
30
31
- 32
33 9. Zhu, M.; Aikens, C. M.; Hendrich, M. P.; Gupta, R.; Qian, H.; Schatz, G. C.; Jin, R.
34
35 Reversible switching of magnetism in thiolate-protected Au₂₅ superatoms. *J. Am. Chem. Soc.*
36
37 **2009**, *131*, 2490-2492.
38
39
- 40
41 10. Antonello, S.; Perera, N. V.; Ruzzi, M.; Gascón, J. A.; Maran, F. Interplay of charge state,
42
43 lability, and magnetism in the molecule-like Au₂₅(SR)₁₈ cluster. *J. Am. Chem. Soc.* **2013**, *135*,
44
45 15585-15594.
46
47
- 48
49 11. Bellon, P.; Manassero, M.; Sansoni, M. An octahedral gold cluster: crystal and molecular
50
51 structure of hexakis[tris-(p-tolyl)phosphine]-octahedro-hexagold bis(tetraphenylborate). *J. Chem.*
52
53 *Soc., Dalton Transactions* **1973**, *22*, 2423-2427.
54
55
56
57
58
59
60

- 1
2
3 12. Bellon, P. L.; Cariati, F.; Manassero, M.; Naldini, L.; Sansoni, M. Novel gold clusters.
4
5 Preparation, properties, and X-ray structure determination of salts of
6
7 octakis(triarylphosphine)enneagold, $[\text{Au}_9\text{L}_8]\text{X}_3$. *J. Chem. Soc., D: Chem. Commun.* **1971**, *22*,
8
9 1423-1424.
10
11
12
13 13. Yao, H.; Iwatsu, M. Water-Soluble Phosphine-Protected Au₁₁ Clusters: Synthesis,
14
15 Electronic Structure, and Chiral Phase Transfer in a Synergistic Fashion. *Langmuir* **2016**, *32*,
16
17 3284-3293.
18
19
20
21 14. Akola, J.; Kacprzak, K. A.; Lopez-Acevedo, O.; Walter, M.; Grönbeck, H.; Häkkinen, H.
22
23 Thiolate-protected Au₂₅ superatoms as building blocks: dimers and crystals. *J. Phys. Chem. C*
24
25 **2010**, *114*, 15986-15994.
26
27
28
29 15. Akola, J.; Walter, M.; Whetten, R. L.; Hakkinen, H.; Gronbeck, H. On the structure of
30
31 thiolate-protected Au₂₅. *J. Am. Chem. Soc.* **2008**, *130*, 3756-3757.
32
33
34
35 16. Walter, M.; Akola, J.; Lopez-Acevedo, O.; Jadzinsky, P. D.; Calero, G.; Ackerson, C. J.;
36
37 Whetten, R. L.; Grönbeck, H.; Häkkinen, H. A unified view of ligand-protected gold clusters as
38
39 superatom complexes. *Proc. Natl Acad. of Sci.* **2008**, *105*, 9157-9162.
40
41
42
43 17. Abdul Halim, L. G.; Ashraf, S.; Katsiev, K.; Kirmani, A. R.; Kothalawala, N.; Anjum, D. H.;
44
45 Abbas, S.; Amassian, A.; Stellacci, F.; Dass, A.; Hussain, I.; Bakr, O. M. A scalable synthesis of
46
47 highly stable and water dispersible Ag₄₄(SR)₃₀ nanoclusters. *J. Mater. Chem. A* **2013**, *1*, 10148-
48
49 10154.
50
51
52
53
54
55
56
57
58
59
60

- 1
2
3 18. AbdulHalim, L. G.; Kothalawala, N.; Sinatra, L.; Dass, A.; Bakr, O. M. Neat and complete:
4 thiolate-ligand exchange on a silver molecular nanoparticle. *J. Am. Chem. Soc.* **2014**, *136*,
5 15865-15868.
6
7
8
9
10
11 19. Yang, H.; Wang, Y.; Huang, H.; Gell, L.; Lehtovaara, L.; Malola, S.; Häkkinen, H.; Zheng,
12 N. All-thiol-stabilized Ag₄₄ and Au₁₂Ag₃₂ nanoparticles with single-crystal structures. *Nat.*
13 *Commun.* **2013**, *4*, 2422.
14
15
16
17
18
19 20. Chakraborty, I.; Kurashige, W.; Kanehira, K.; Gell, L.; Häkkinen, H.; Negishi, Y.; Pradeep,
20 T. Ag₄₄(SeR)₃₀: A Hollow Cage Silver Cluster with Selenolate Protection. *J. Phys. Chem. Lett.*
21 **2013**, *4*, 3351-3355.
22
23
24
25
26
27 21. Kurashige, W.; Yamaguchi, M.; Nobusada, K.; Negishi, Y. Ligand-Induced Stability of Gold
28 Nanoclusters: Thiolate versus Selenolate. *J. Phys. Chem. Lett.* **2012**, *3*, 2649-2652.
29
30
31
32 22. Ossowski, J.; Wächter, T.; Silies, L.; Kind, M.; Noworolska, A.; Blobner, F.; Gnatek, D.;
33 Rysz, J.; Bolte, M.; Feulner, P.; Terfort, A.; Cyganik, P.; Zharnikov, M. Thiolate versus
34 Selenolate: Structure, Stability, and Charge Transfer Properties. *ACS Nano* **2015**, *9*, 4508-4526.
35
36
37
38
39
40 23. Maity, P.; Takano, S.; Yamazoe, S.; Wakabayashi, T.; Tsukuda, T. Binding motif of terminal
41 alkynes on gold clusters. *J. Am. Chem. Soc.* **2013**, *135*, 9450-9457.
42
43
44
45
46 24. Templeton, A. C.; Wuelfing, W. P.; Murray, R. W. Monolayer-protected cluster molecules.
47 *Acc. Chem. Res.* **2000**, *33*, 27-36.
48
49
50
51 25. Hannu Häkkinen The gold–sulfur interface at the nanoscale *Nat. Chem.* **2012**, *4*, 443–455.
52
53
54
55
56
57
58
59
60

- 1
2
3 26. Häkkinen, H.; Walter, M.; Grönbeck, H. Divide and Protect: Capping Gold Nanoclusters
4 with Molecular Gold–Thiolate Rings. *J. Phys. Chem. B* **2006**, *110*, 9927-9931.
5
6
7
8
9 27. Walter, M.; Akola, J.; Lopez-Acevedo, O.; Jadzinsky, P. D.; Calero, G.; Ackerson, C. J.;
10 Whetten, R. L.; Grönbeck, H.; Häkkinen, H. A unified view of ligand-protected gold clusters as
11 superatom complexes. *Proc Nat. Acad. Sci.* **2008**, *105*, 9157-9162.
12
13
14
15
16 28. Natarajan, G.; Mathew, A.; Negishi, Y.; Whetten, R. L.; Pradeep, T. A unified framework for
17 understanding the structure and modifications of atomically precise monolayer protected gold
18 clusters. *J. Phys. Chem. C* **2015**, *119*, 27768-27785.
19
20
21
22
23
24 29. Yamazoe, S.; Takano, S.; Kurashige, W.; Yokoyama, T.; Nitta, K.; Negishi, Y.; Tsukuda, T.
25 Hierarchy of bond stiffnesses within icosahedral-based gold clusters protected by thiolates. *Nat.*
26 *Commun.* **2016**, *7*, 10414.
27
28
29
30
31
32 30. Tlahuice-Flores, A.; Black, D. M.; Bach, S. B. H.; Jose-Yacaman, M.; Whetten, R. L.
33 Structure & bonding of the gold-subhalide cluster I-Au₁₄₄Cl₆₀^[Z]. *Phys. Chem. Chem. Phys.* **2013**,
34 *15*, 19191-19195.
35
36
37
38
39
40 31. Chen, Y.; Zeng, C.; Kauffman, D. R.; Jin, R. Tuning the Magic Size of Atomically Precise
41 Gold Nanoclusters via Isomeric Methylbenzenethiols. *Nano Lett.* **2015**, *15*, 3603–3609.
42
43
44
45
46 32. Rambukwella, M.; Sakthivel, N. A.; Delcamp, J. H.; Sementa, L.; Fortunelli, A.; Dass, A.
47 Ligand Structure Determines Nanoparticles' Atomic Structure, Metal-Ligand Interface and
48 Properties. *Front. Chem.* **2018**, *6*, 330.
49
50
51
52
53
54
55
56
57
58
59
60

- 1
2
3 33. Zeng, C.; Qian, H.; Li, T.; Li, G.; Rosi, N. L.; Yoon, B.; Barnett, R. N.; Whetten, R. L.;
4
5 Landman, U.; Jin, R. Total Structure and Electronic Properties of the Gold Nanocrystal
6
7 $\text{Au}_{36}(\text{SR})_{24}$. *Angew. Chem. Int. Ed.* **2012**, *51*, 13114–13118.
8
9
10
11 34. Dolamic, I.; Knoppe, S.; Dass, A.; Bürgi, T. First enantioseparation and circular dichroism
12
13 spectra of Au_{38} clusters protected by achiral ligands. *Nat. Commun.* **2012**, *3*, 798.
14
15
16
17 35. Dolamic, I.; Varnholt, B.; Bürgi, T. Chirality transfer from gold nanocluster to adsorbate
18
19 evidenced by vibrational circular dichroism. *Nat. Commun.* **2015**, *6*, 7117.
20
21
22
23 36. Mathew, A.; Natarajan, G.; Lehtovaara, L.; Häkkinen, H.; Kumar, R. M.; Subramanian, V.;
24
25 Jaleel, A.; Pradeep, T. Supramolecular functionalization and concomitant enhancement in
26
27 properties of Au_{25} clusters. *ACS Nano* **2014**, *8*, 139-152.
28
29
30
31 37. Yoon, B.; Luedtke, W. D.; Barnett, R. N.; Gao, J.; Desireddy, A.; Conn, B. E.; Bigioni, T.;
32
33 Landman, U. Hydrogen-bonded structure and mechanical chiral response of a silver nanoparticle
34
35 superlattice. *Nat. Mater.* **2014**, *13*, 807-811.
36
37
38
39 38. De Nardi, M.; Antonello, S.; Jiang, D.-e.; Pan, F.; Rissanen, K.; Ruzzi, M.; Venzo, A.; Zoleo,
40
41 A.; Maran, F. Gold nanowired: a linear $(\text{Au}_{25})_n$ polymer from Au_{25} molecular clusters. *ACS Nano*
42
43 **2014**, *8*, 8505-8512.
44
45
46
47 39. Som, A.; Chakraborty, I.; Maark, T. A.; Bhat, S.; Pradeep, T. Cluster-mediated crossed
48
49 bilayer precision assemblies of 1D nanowires. *Adv. Mater.* **2016**, *28*, 2827-2833.
50
51
52 40. Gell, L.; Häkkinen, H. Theoretical analysis of the $\text{M}_{12}\text{Ag}_{32}(\text{SR})_{40}^{4-}$ and $\text{X}@\text{M}_{12}\text{Ag}_{32}(\text{SR})_{30}^{4-}$
53
54 nanoclusters (M = Au, Ag; X = H, Mn). *J. Phys. Chem. C* **2015**, *119*, 10943-10948.
55
56
57
58
59
60

- 1
2
3 41. Wu, Z.; Jin, R. On the ligand's role in the fluorescence of gold nanoclusters. *Nano Lett.* **2010**,
4
5 *10*, 2568-2573.
6
7
8
9 42. Mathew, A.; Varghese, E.; Choudhury, S.; Pal, S. K.; Pradeep, T. Efficient red luminescence
10 from organic-soluble Au₂₅ clusters by ligand structure modification. *Nanoscale* **2015**, *7*, 14305-
11 14315.
12
13
14
15
16 43. Niihori, Y.; Kikuchi, Y.; Kato, A.; Matsuzaki, M.; Negishi, Y. Understanding ligand-
17 exchange reactions on thiolate-protected gold clusters by probing isomer distributions using
18 reversed-phase high-performance liquid chromatography. *ACS Nano* **2015**, *9*, 9347-9356.
19
20
21
22
23
24 44. Ni, T. W.; Tofanelli, M. A.; Phillips, B. D.; Ackerson, C. J. Structural basis for ligand
25 exchange on Au₂₅(SR)₁₈. *Inorg. Chem.* **2014**, *53*, 6500-6502.
26
27
28
29
30 45. Dass, A.; Holt, K.; Parker, J. F.; Feldberg, S. W.; Murray, R. W. Mass spectrometrically
31 detected statistical aspects of ligand populations in mixed monolayer Au₂₅L₁₈ nanoparticles. *J.*
32 *Phys. Chem. C* **2008**, *112*, 20276-20283.
33
34
35
36
37
38 46. Song, Y.; Huang, T.; Murray, R. W. Heterophase ligand exchange and metal transfer
39 between monolayer protected clusters. *J. Am. Chem. Soc.* **2003**, *125*, 11694-11701.
40
41
42
43
44 47. Song, Y.; Murray, R. W. Dynamics and extent of ligand exchange depend on electronic
45 charge of metal nanoparticles. *J. Am. Chem. Soc.* **2002**, *124*, 7096-7102.
46
47
48
49 48. Wang, S.; Song, Y.; Jin, S.; Liu, X.; Zhang, J.; Pei, Y.; Meng, X.; Chen, M.; Li, P.; Zhu, M.
50 Metal exchange method using Au₂₅ nanoclusters as templates for alloy nanoclusters with atomic
51 precision. *J. Am. Chem. Soc.* **2015**, *137*, 4018-4021.
52
53
54
55
56
57
58
59
60

- 1
2
3 49. Krishnadas, K. R.; Udayabhaskararao, T.; Choudhury, S.; Goswami, N.; Pal, S. K.; Pradeep,
4
5 T. Luminescent AgAu alloy clusters derived from Ag nanoparticles - Manifestations of tunable
6
7 Au(I)-Cu(I) metallophilic interactions. *Eur. J. Inorg. Chem.* **2014**, *2014*, 908-916.
8
9
10
11 50. Walter, M.; Moseler, M., Ligand-protected gold alloy clusters: doping the superatom. *J.*
12
13 *Phys. Chem. C* **2009**, *113*, 15834-15837.
14
15
16
17 51. Tian, S.; Yao, C.; Liao, L.; Xia, N.; Wu, Z. Ion-precursor and ion-dose dependent anti-
18
19 galvanic reduction. *Chem. Commun.* **2015**, *51*, 11773-11776.
20
21
22
23 52. Wu, Z. Anti-Galvanic reduction of thiolate-protected gold and silver nanoparticles. *Angew.*
24
25 *Chem. Int. Ed.* **2012**, *51*, 2934-2938.
26
27
28 53. Udayabhaskararao, T.; Sun, Y.; Goswami, N.; Pal, S. K.; Balasubramanian, K.; Pradeep, T.
29
30 Ag₇Au₆: A 13-atom alloy quantum cluster. *Angew. Chem. Int. Ed.* **2012**, *51*, 2155-2159.
31
32
33
34 54. Dreier, T. A.; Ackerson, C. J. Radicals are required for thiol etching of gold particles. *Angew.*
35
36 *Chem. Int. Ed.* **2015**, *54*, 9249-9252.
37
38
39 55. Udaya Bhaskara Rao, T.; Pradeep, T. Luminescent Ag₇ and Ag₈ clusters by interfacial
40
41 synthesis. *Angew. Chem. Int. Ed.* **2010**, *49*, 3925-3929.
42
43
44
45 56. Shichibu, Y.; Negishi, Y.; Tsukuda, T.; Teranishi, T. Large-scale synthesis of thiolated Au₂₅
46
47 clusters via ligand exchange reactions of phosphine-stabilized Au₁₁ clusters. *J. Am. Chem. Soc.*
48
49 **2005**, *127*, 13464-13465.
50
51
52
53
54
55
56
57
58
59
60

- 1
2
3 57. Shichibu, Y.; Negishi, Y.; Watanabe, T.; Chaki, N. K.; Kawaguchi, H.; Tsukuda, T.
4
5 Biicosahedral gold clusters $[\text{Au}_{25}(\text{PPh}_3)_{10}(\text{SC}_n\text{H}_{2n+1})_5\text{Cl}_2]^{2+}$ ($n = 2-18$): A stepping stone to
6
7 cluster-assembled materials. *J. Phys. Chem. C* **2007**, *111*, 7845-7847.
8
9
10
11 58. Li, M.-B.; Tian, S.-K.; Wu, Z.; Jin, R. Peeling the core-shell Au_{25} nanocluster by reverse
12
13 ligand-exchange. *Chem. Mater.* **2016**, *28*, 1022-1025.
14
15
16
17 59. Krishnadas, K. R.; Baksi, A.; Ghosh, A.; Natarajan, G.; Pradeep, T. Structure-conserving
18
19 spontaneous transformations between nanoparticles. *Nat. Commun.* **2016**, *7*, 13447.
20
21
22
23 60. Krishnadas, K. R.; Baksi, A.; Ghosh, A.; Natarajan, G.; Pradeep, T. Manifestation of
24
25 Geometric and Electronic Shell Structures of Metal Clusters in Intercluster Reactions. *ACS Nano*
26
27 **2017**, *11*, 6015-6023.
28
29
30
31 61. Krishnadas, K. R.; Baksi, A.; Ghosh, A.; Natarajan, G.; Som, A.; Pradeep, T. Interparticle
32
33 Reactions: An Emerging Direction in Nanomaterials Chemistry. *Acc. Chem. Res.* **2017**, *50*,
34
35 1988-1996.
36
37
38
39 62. Krishnadas, K. R.; Ghosh, A.; Baksi, A.; Chakraborty, I.; Natarajan, G.; Pradeep, T.
40
41 Intercluster reactions between $\text{Au}_{25}(\text{SR})_{18}$ and $\text{Ag}_{44}(\text{SR})_{30}$. *J. Am. Chem. Soc.* **2016**, *138*, 140-148.
42
43
44
45 63. Zhang, B.; Salassa, G.; Burgi, T. Silver migration between $\text{Au}_{38}(\text{SC}_2\text{H}_4\text{Ph})_{24}$ and doped
46
47 $\text{Ag}_x\text{Au}_{38-x}(\text{SC}_2\text{H}_4\text{Ph})_{24}$ nanoclusters. *Chem. Commun.* **2016**, *52*, 9205-9207.
48
49
50
51 64. Xia, N.; Wu, Z. Doping Au_{25} nanoparticles using ultrasmall silver or copper nanoparticles as
52
53 the metal source. *J. Mater. Chem. C* **2016**, *4*, 4125-4128.
54
55
56
57
58
59
60

- 1
2
3 65. Bootharaju, M. S.; Sinatra, L.; Bakr, O. M. Distinct metal-exchange pathways of doped Ag₂₅
4 nanoclusters. *Nanoscale* **2016**, *8*, 17333-17339.
5
6
7
8
9 66. Zhang, B.; Safonova, O. V.; Pollitt, S.; Salassa, G.; Sels, A.; Kazan, R.; Wang, Y.;
10 Rupprechter, G.; Barrabes, N.; Burgi, T. On the mechanism of rapid metal exchange between
11 thiolate-protected gold and gold/silver clusters: a time-resolved in situ XAFS study. *Phys. Chem.*
12 *Chem. Phys.* **2018**, *20*, 5312-5318.
13
14
15
16
17
18
19 67. Yao, Q.; Feng, Y.; Fung, V.; Yu, Y.; Jiang, D.-e.; Yang, J.; Xie, J. Precise control of alloying
20 sites of bimetallic nanoclusters via surface motif exchange reaction. *Nat. Commun.* **2017**, *8*,
21 1555.
22
23
24
25
26
27 68. Wang, S.; Abroshan, H.; Liu, C.; Luo, T.-Y.; Zhu, M.; Kim, H. J.; Rosi, N. L.; Jin, R.
28 Shuttling single metal atom into and out of a metal nanoparticle. *Nat. Commun.* **2017**, *8*, 848.
29
30
31
32
33 69. Varnholt, B.; Oulevey, P.; Lubber, S.; Kumara, C.; Dass, A.; Bürgi, T. Structural Information
34 on the Au–S Interface of Thiolate-Protected Gold Clusters: A Raman Spectroscopy Study. *J.*
35 *Phys. Chem. C* **2014**, *118*, 9604-9611.
36
37
38
39
40
41 70. Burgi, T. Properties of the gold-sulphur interface: from self-assembled monolayers to
42 clusters. *Nanoscale* **2015**, *7*, 15553-15567.
43
44
45
46
47 71. Salassa, G.; Sels, A.; Mancin, F.; Bürgi, T. Dynamic Nature of Thiolate Monolayer in
48 Au₂₅(SR)₁₈ Nanoclusters. *ACS Nano* **2017**, *11*, 12609-12614.
49
50
51
52
53
54
55
56
57
58
59
60

- 1
2
3 72. Salorinne, K.; Malola, S.; Wong, O. A.; Rithner, C. D.; Chen, X.; Ackerson, C. J.; Häkkinen,
4 H. Conformation and dynamics of the ligand shell of a water-soluble Au₁₀₂ nanoparticle. *Nat.*
5
6 *Commun.* **2016**, *7*, 10401.
7
8
9
10
11 73. Ouyang, R.; Jiang, D.-e. Ligand-Conformation Energy Landscape of Thiolate-Protected Gold
12
13 Nanoclusters. *J. Phys. Chem. C* **2015**, *119*, 21555-21560.
14
15
16
17 74. Pradeep, T.; Mitra, S.; Nair, A. S.; Mukhopadhyay, R. Dynamics of alkyl chains in
18
19 monolayer-protected Au and Ag clusters and silver thiolates: a comprehensive quasielastic
20
21 neutron scattering investigation. *J. Phys. Chem. B* **2004**, *108*, 7012-7020.
22
23
24
25 75. Khatun, E.; Ghosh, A.; Ghosh, D.; Chakraborty, P.; Nag, A.; Mondal, B.; Chennu, S.;
26
27 Pradeep, T. [Ag₅₉(2,5-DCBT)₃₂]³⁻: a new cluster and a precursor for three well-known clusters.
28
29 *Nanoscale* **2017**, *9*, 8240-8248.
30
31
32
33 76. Baksi, A.; Ghosh, A.; Mudedla, S. K.; Chakraborty, P.; Bhat, S.; Mondal, B.; Krishnadas, K.
34
35 R.; Subramanian, V.; Pradeep, T. Isomerism in Monolayer Protected Silver Cluster Ions: An Ion
36
37 Mobility-Mass Spectrometry Approach. *J. Phys. Chem. C* **2017**, *121*, 13421-13427.
38
39
40
41 77. Baksi, A.; Chakraborty, P.; Bhat, S.; Natarajan, G.; Pradeep, T. [Au₂₅(SR)₁₈]₂²⁻: a noble metal
42
43 cluster dimer in the gas phase. *Chem. Commun.* **2016**, *52*, 8397-8400.
44
45
46
47 78. Ghosh, A.; Bodiuzzaman, M.; Nag, A.; Jash, M.; Baksi, A.; Pradeep, T. Sequential
48
49 Dihydrogen Desorption from Hydride-Protected Atomically Precise Silver Clusters and the
50
51 Formation of Naked Clusters in the Gas Phase. *ACS Nano* **2017**, *11*, 11145-11151.
52
53
54
55
56
57
58
59
60

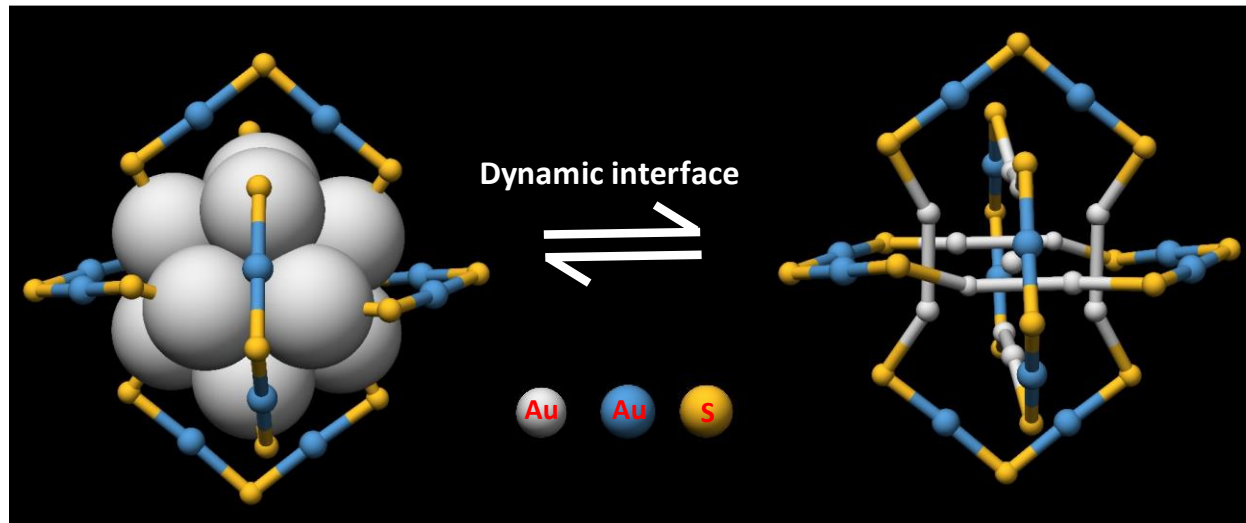
- 1
2
3 79. Krishnadas., K. R.; Thumu, U.; Susobhan, C.; Nirmal, G.; Kumar, P. S.; Thalappil, P.
4 Luminescent AgAu Alloy Clusters Derived from Ag Nanoparticles – Manifestations of Tunable
5 AuI–CuI Metallophilic Interactions. *Eur. J. Inorg. Chem.* **2014**, *2014*, 908-916.
6
7
8
9
10
11 80. Wang, S.; Song, Y.; Jin, S.; Liu, X.; Zhang, J.; Pei, Y.; Meng, X.; Chen, M.; Li, P.; Zhu, M.
12 Metal Exchange Method Using Au₂₅ Nanoclusters as Templates for Alloy Nanoclusters with
13 Atomic Precision. *J. Am. Chem. Soc.* **2015**, *137*, 4018-4021.
14
15
16
17
18
19 81. Wiseman, M. R.; Marsh, P. A.; Bishop, P. T.; Brisdon, B. J.; Mahon, M. F. Homoleptic Gold
20 Thiolate Catenanes. *J. Am. Chem. Soc.* **2000**, *122*, 12598–12599.
21
22
23
24 82. Zeng, C.; Liu, C.; Chen, Y.; Rosi, N. L.; Jin, R. Gold-Thiolate Ring as a Protecting Motif in
25 the Au₂₀(SR)₁₆ Nanocluster and Implications. *J. Am. Chem. Soc.* **2014**, *136*, 11922–11925.
26
27
28
29
30 83. Yan, N.; Xia, N.; Liao, L.; Zhu, M.; Jin, F.; Jin, R.; Wu, Z. Unraveling the long-pursued
31 Au₁₄₄ structure by x-ray crystallography. *Science Advances* **2018**, *4*, 7259.
32
33
34
35
36 84. Ghosh, A.; Ghosh, D.; Khatun, E.; Chakraborty, P.; Pradeep, T. Unusual reactivity of dithiol
37 protected clusters in comparison to monothiol protected clusters: studies using
38 Ag₅₁(BDT)₁₉(TPP)₃ and Ag₂₉(BDT)₁₂(TPP)₄. *Nanoscale* **2017**, *9*, 1068-1077.
39
40
41
42
43 85. Viswanatha, R.; Sarma, D. D. *Growth of Nanocrystals in Solution* In, Nanomaterials
44 Chemistry Ed. C.N.R. Rao, A. Müller, and A.K. Cheetham, 2007, WILEY-VCH Verlag GmbH
45 & Co. KGaA, Weinheim.
46
47
48
49
50
51
52
53
54
55
56
57
58
59
60

- 1
2
3 86. Dainese, T.; Antonello, S.; Bogialli, S.; Fei, W.; Venzo, A.; Maran, F. Gold Fusion: From
4 Au₂₅(SR)₁₈ to Au₃₈(SR)₂₄, the Most Unexpected Transformation of a Very Stable Nanocluster
5
6 *ACS Nano* **2018**, *12*, 7057–7066.
7
8
9
10
11 87. Guo, R.; Song, Y.; Wang, G.; Murray, R. W. Does core size matter in the kinetics of ligand
12 exchanges of monolayer-protected Au clusters? *J. Am. Chem. Soc.* **2005**, *127*, 2752-2757.
13
14
15
16
17 88. Bootharaju, M. S.; Burlakov, V. M.; Besong, T. B. D.; Joshi, C. P.; AbdulHalim, L. G.;
18 Black, D. M.; Whetten, R. L.; Goriely, A.; Bakr, O. M. Reversible Size Control of Silver
19 Nanoclusters via Ligand-Exchange. *Chem. Mater.* **2015**, *27*, 4289–4297.
20
21
22
23
24 89. Bootharaju, M. S.; Joshi, C. P.; Alhilaly, M. J.; Bakr, O. M. Switching a nanocluster core
25 from hollow to nonhollow. *Chem. Mater.* **2016**, *28*, 3292-3297.
26
27
28
29
30 90. Laphorn, C.; Pullen, F.; Chowdhry, B. Z. Ion mobility spectrometry-mass spectrometry (IMS-
31 MS) of small molecules: separating and assigning structures to ions. *Mass Spectrometry Reviews*,
32
33 **2013**, *32*, 43–71.
34
35
36
37
38 91. Angel, L. A.; Majors, L. T.; Dharmaratne, A. C.; Dass, A. Ion mobility mass spectrometry of
39 Au₂₅(SCH₂CH₂Ph)₁₈ nanoclusters. *ACS Nano* **2010**, *4*, 4691-4700.
40
41
42
43
44 92. Chakraborty, P.; Baksi, A.; Khatun, E.; Nag, A.; Ghosh, A.; Pradeep, T. Dissociation of Gas
45 Phase Ions of Atomically Precise Silver Clusters Reflects Their Solution Phase Stability. *J. Phys.*
46 *Chem. C* **2017**, *121*, 10971-10981.
47
48
49
50
51 93. Liu, C.; Lin, S.; Pei, Y.; Zeng, X. C. Semiring chemistry of Au₂₅(SR)₁₈: Fragmentation
52 pathway and catalytic active site. *J. Am. Chem. Soc.* **2013**, *135*, 18067-18079.
53
54
55
56
57
58
59
60

1
2
3 94. Jash, M.; Reber, A. C.; Ghosh, A.; Sarkar, D.; Bodiuzzaman, M.; Basuri, P.; Baksi, A.;
4
5 Khanna, S. N.; Pradeep, T. Preparation of gas phase naked silver cluster cations outside the mass
6
7 spectrometer from ligand protected clusters in solution. *Nanoscale* **2018**, *10*, 15714–15722.
8
9
10
11
12
13
14
15
16
17
18
19
20
21
22
23
24
25
26
27
28
29
30
31
32
33
34
35
36
37
38
39
40
41
42
43
44
45
46
47
48
49
50
51
52
53
54
55
56
57
58
59
60

1
2
3
4
5
6
7
8
9
10
11
12
13
14
15
16
17
18
19
20
21
22
23
24
25
26
27
28
29
30
31
32
33
34
35
36
37
38
39
40
41
42
43
44
45
46
47
48
49
50
51
52
53
54
55
56
57
58
59
60

Image for the Table of Contents



Biographies



Krishnadas, after earning a Ph.D. in Chemistry from the Indian Institute of Technology Madras in 2016 under the guidance of Prof. T. Pradeep, is currently a postdoctoral researcher at University of Geneva, Switzerland. He explores chemical reactions of atomically precise noble metal clusters.



Ganapati Natarajan, after earning a Ph.D. in Chemistry (2011) from the Department of Chemistry at the University of Cambridge, UK, is a postdoctoral researcher in Prof. Pradeep's research group. He is a computational materials scientist with interests in structure and properties of ligand-protected noble metal clusters and nanoparticles, ice, amorphous materials, and materials and nanomaterials in general.



13
14 Ananya Baksi, after earning a Ph.D. in Chemistry from the Indian Institute of Technology Madras
15 in 2015 under the guidance of Prof. T. Pradeep, is currently a postdoctoral researcher at Karlsruhe
16 Institute of Technology, Germany. Her research is focused on mass spectrometric investigations
17 of different cluster systems.
18
19
20
21
22



36 Atanu Ghosh after earning a Ph.D. in Chemistry from the Indian Institute of Technology Madras
37 in 2015 under the guidance of Prof. T. Pradeep, is currently a postdoctoral researcher at King
38 Abdullah University of Science and Technology, Saudi Arabia. His research focuses on the
39 synthesis, reactions, and applications of noble metal nanoclusters.
40
41
42
43
44
45
46
47
48
49
50
51
52
53
54
55
56
57
58
59
60



1
2
3
4
5
6
7
8
9
10
11
12
13
14
15
16
17 Esma Khatun is a Ph.D. student of Prof. T. Pradeep at the Dept. of Chemistry, Indian Institute of
18 Technology Madras, India. Her research focuses on the synthesis, reactions, and applications of
19 noble metal nanoclusters.
20
21
22
23

24
25 T. Pradeep is an Institute Professor and Deepak Parekh Institute Chair Professor at the Indian
26 Institute of Technology Madras. Prof. Pradeep's research interests are in molecular and nanoscale
27 materials, and he develops instrumentation for such studies. He is involved in the development of
28 affordable technologies for drinking water purification, and some of his technologies have been
29 commercialized.
30
31
32
33
34
35
36
37
38
39
40
41
42
43
44
45
46
47
48
49
50
51
52
53
54
55
56
57
58
59
60